Electropneumotactile Stimulation: Multimodal Haptic Actuators Enabled by a Stretchable Conductive Polymer on Inflatable Pockets

Cody W. Carpenter, Marigold G. Malinao, Tarek A. Rafeedi, Daniel Rodriquez, Siew Ting Melissa Tan, Nicholas B. Root, Kyle Skelil, Julian Ramírez, Beril Polat, Samuel E. Root, Vilayanur S. Ramachandran, and Darren J. Lipomi*

A type of haptic device is described that delivers two modes of stimulation simultaneously and at the same location on the skin. The two modes of stimulation are mechanical (delivered pneumatically by inflatable air pockets embedded within a silicone elastomer) and electrical (delivered by a conductive polymer). The key enabling aspect of this work is the use of a highly plasticized conductive polymer based on poly(3,4-ethylenedioxythiphene) (PEDOT) blended with elastomeric polyurethane (PU). To fabricate the "electropneumotactile" device, the polymeric electrodes are overlaid directly on top of the elastomeric pneumatic actuator pockets. Co-placement of the pneumatic actuators and the electrotactile electrodes is enabled by the stretchability of the PEDOT:tosylate/PU blend, allowing the electrotactiles to conform to underlying pneumatic pockets under deformation. The blend of PEDOT and PU has a Young's modulus of ≈150 MPa with little degradation in conductivity following repeated inflation of the air pockets. The ability to perceive simultaneous delivery of two sensations to the same location on the skin is supported by experiments using human subjects. These results show that participants can successfully detect the location of pneumatic stimulation and whether electrotactile stimulation is delivered (yes/no) at a rate significantly above chance (mean accuracy = 94%).

The ability to simulate complex tactile sensations in a wearable haptic device in virtual and augmented reality (VR and AR) depends on the ability to put the active components in the same location. In analogy to a pixel in a visual display that contains subpixels for red, green, and blue, it would be similarly advantageous to fabricate tactile pixels capable of delivering more than one type of sensation. In this study, we use inflatable air pockets coated with a stretchable conductive polymer to enable simultaneous mechanical and electrical stimulation in the same location on the skin. We call this type of mixed-mode device an "electropneumotactile" actuator (**Figure 1**). Specifically, inflatable pockets were fabricated in slabs of poly(dimethylsiloxane) (PDMS) and overlaid with patterned electrodes made of a blend of poly(3,4-ethylenedioxythiophene) and tosylate (PEDOT:OTs) and elastomeric polyurethane (PU, Figure 1).[1] Blending of the conductive polymer with the elastomer permitted the electrodes to remain intact upon repeated inflation of the underlying air pockets. Upon pressurization, the air pockets were inflated with vertical displacements of ≥1 mm, which were perceived as a bumpy topography or vibration of a virtual surface, depending on whether the state of inflation was static or periodic. In contrast, the electrical—electrotactile— modality can be made to feel tingly or to mimic (approximately) the fine texture of surfaces. Experiments using human subjects confirmed that it was possible to differentiate these sensations when delivered simultaneously. Such a capability could be useful for applications needing to recapitulate more than one property of a surface at the same time. This demonstration is part of an effort to use the tools of organic materials chemistry in haptics research—"organic haptics."[2–4,5]

Multimodal haptic actuators may play a key role in future haptic devices for VR and AR. Examples of approaches for realizing multimodal haptic stimulation include the combination of vibrotactile devices and electrotactile stimulators for mechanical and electrical stimulation,[6] electrostatic and vibrotactile stimulators for variable friction and vibrational surfaces,[7] and thermal and vibrotactile stimulators for temperature and vibrational feedback.[7] Two types of haptic effect that have not been previously combined are pneumatic and electrotactile stimulation. Ideally, these stimulators would occupy the same physical location in order to 1) save space and 2) produce mixed modes

Dr. C. W. Carpenter, M. G. Malinao, T. A. Rafeedi, Dr. D. Rodriquez, S. T. M. Tan, K. Skelil, J. Ramírez, B. Polat, Dr. S. E. Root, Prof. D. J. Lipomi
Department of NanoEngineering
University of California, San Diego
9500 Gilman Drive, Mail Code 0448, La Jolla, CA 92093-0448, USA
E-mail: dlipomi@eng.ucsd.edu
Dr. N. B. Root, Prof. V. S. Ramachandran
Department of Psychology
University of California, San Diego
9500 Gilman Drive, Mail Code 0109, La Jolla, CA 92093-0109, USA

The ORCID identification number(s) for the author(s) of this article can be found under https://doi.org/10.1002/admt.201901119.
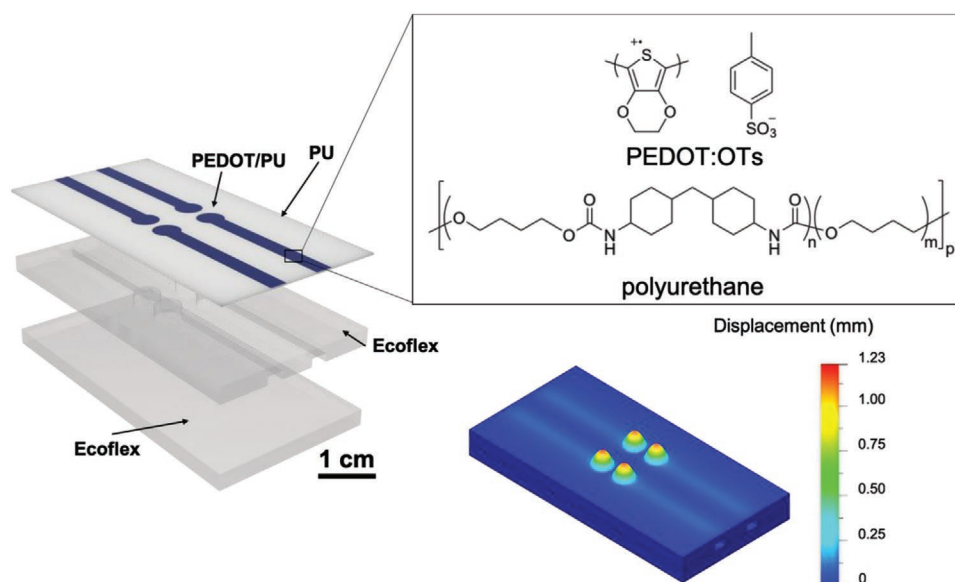
Figure 1. Schematic drawing of a multimodal haptic actuator comprising stretchable electrotactile stimulators (PEDOT:OTs/PU) superimposed on pneumatic actuators (Ecoflex silicone elastomer). Inset: Chemical structures of ethylenedioxythiophene with tosylate and PU. Bottom: Finite element analysis of four pneumatic pixels used to simulate the magnitude of displacement of each pocket when inflated.

of stimulation. That is, the electrodes used for electrotactile stimulation should be placed on top of the pneumatic pockets. While metals would be the intuitive choice for the material to supply the electrical stimulation, solid metals fracture at strains much smaller than those expected to be produced upon inflation of the pockets.

Pneumatic actuators have been explored for a wide variety of applications in haptics.[8] For example, they can be arranged into pixelated arrays for reconfigurable Braille displays.[9,10] While pneumatic actuators typically comprise an air pocket in an elastomer,[9,11] the use of other materials and components can add functionality, such as the ability to "lock" the pixels into place. For example, Soule and Lazarus demonstrated a pneumatic Braille array whose configuration could be locked into place by filling the pockets with low-melting-point alloys.[9] In another example, Besse et al. achieved a similar result in a 32 × 24 array using a shape-memory polymer. Individual pixels were softened using stretchable heaters prior to inflation.[12] It is also possible to affect pneumatic-like displacements using pockets filled with thermally expandable fluids.[11] The advantage of thermal expansion as opposed to inflation is that actuation can be affected using metallic joule heaters powered by on-board batteries instead of bulky air compressors and control valves. The disadvantage of such an approach is low speed of actuation.

Electrotactile stimulation is a form of sensory substitution that uses an alternating current (≈2–4 mA) to stimulate nerve endings in the skin.[13] Electrotactile stimulators operate by way of capacitive coupling between an electrical conductor and ions in sweat to excite mechanoreceptors (neurons responsible for detecting mechanical forces) and nociceptors (responsible for signaling pain). Electrotactile stimulators are used as sensory substitution systems for the blind,[14,15] tactile interfaces within prosthetic limbs for amputees,[16–18] as well as muscle stimulators to reduce pain noninvasively.[19] The most basic

form of electrode for stimulation is a solid metal wire or foil. In order to enable conformability when worn on the skin, soft materials and device layouts that confer stretchability are required. For example, the Rogers laboratory has used metallic electrodes connected by stretchable serpentine interconnects to affect electrotactile stimulation on the interior surface of a silicone thimble.[20] Intrinsically stretchable conductors and conductive composites have also demonstrated usefulness in electrotactile devices. For example, devices employing thin Ag/AgCl electrodes coated with conductive gels have been used in flexible electrotactile devices.[16–18] Materials such as carbon black-filled PDMS have been used successfully for a variety of applications in haptics and soft robotics.[21] Other soft materials used for electrotactile stimulation include graphene[22] and ionically conductive organogels.[23]

π-Conjugated (conductive) polymers are attractive for use as electrotactile devices because of their synthetic tunability, ease of fabrication, and the potential for biocompatibility. However, most π-conjugated polymers that are chemically oxidized ("doped") to achieve metal-like conductivities are nearly as brittle as work-hardened metals, with failure strains of a few percent or less.[24] The mechanical stiffness of conductive polymers can be reduced by the use of additives or covalent modifications to the polymer. For example, the stretchability of PEDOT polymerized around a polyelectrolyte scaffold of poly(styrene sulfonate) (PEDOT:PSS) may be increased by the addition of surfactants such as capstone and Triton X-100,[25] by blending with elastomers such as PU[1] (used in this study), or through chemical modification of the PSS backbone.[24,26] The conductivity of PEDOT:PSS can be improved by addition of high-boiling point solvents, such as dimethyl sulfoxide and ethylene glycol, which also have the effect of plasticizing the polymer.[24] In addition to mechanical deformability, PEDOT:PSS has the advantage of low electrical impedance when used in a biological context (i.e.,
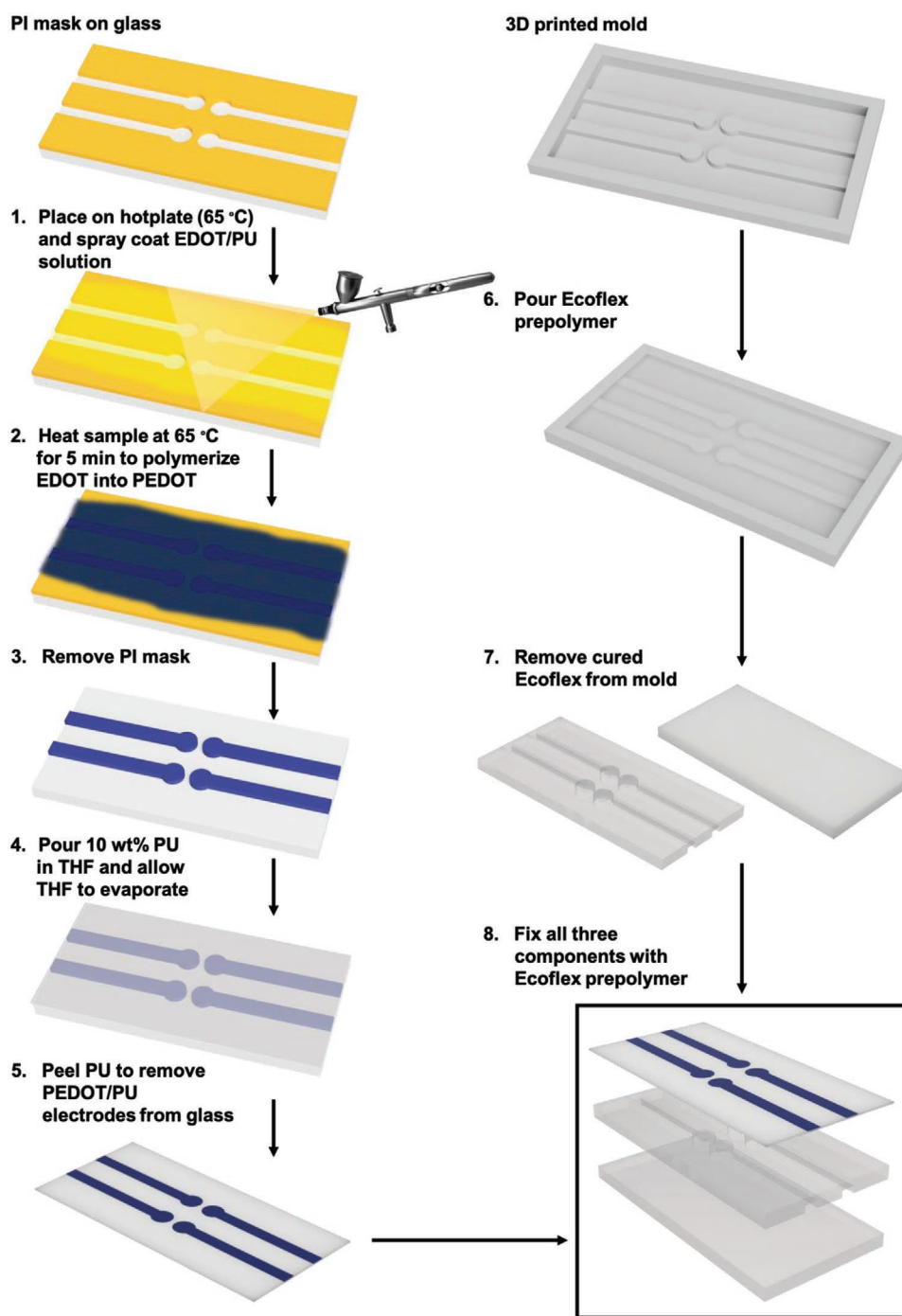
**ADVANCED
SCIENCE NEWS**

www.advancedsciencenews.com

**ADVANCED
MATERIALS
TECHNOLOGIES**

www.advmattechnol.de

Figure 2. Schematic summary of the process used to fabricate the electropneumotactile array.

to stimulate neurons).[27–30] The reduced impedance of metallic electrodes coated with PEDOT:PSS derives from its 3D structure, which increases in the number of ions that capacitively couple at the electrode-electrolyte interface compared to an uncoated metallic electrode. Moreover, PEDOT:PSS and similar formulations can be processed easily from aqueous solution and have good transparency at thicknesses <100 nm.[31]

The stretchable electrotactile and pneumatic actuators were combined using the fabrication scheme depicted in **Figure 2**.

The electropneumotactile device comprised four PEDOT:OTs/PU electrodes supported on a PU substrate and four pneumatic pixels made of Ecoflex silicone elastomer. This formulation was chosen due to its favorable combination of conductivity and stretchability. The electrodes were patterned by spray coating a 10 µm layer of PEDOT:OTs/PU through a polyimide (PI) mask on glass while heating on a hotplate at 65 °C (steps 1–2). After heating for 5 min, the solution transitioned from a translucent yellow to an opaque blue once the EDOT fully polymerized into

**ADVANCED
SCIENCE NEWS**

www.advancedsciencenews.com

**ADVANCED
MATERIALS
TECHNOLOGIES**

www.advmattechnol.de

PEDOT and the excess solvent evaporated. Next, the sample was submerged in boiling deionized water for 2 s and then in room temperature (22 °C) deionized water to remove iron species used in the polymerizaion of EDOT (not pictured). The PI mask was then removed (step 3). The exposed electrodes were then coated with a thin layer of PU dissolved in tetrahydrofuran (THF). The sample was kept in a fume hood for 10 h to allow the THF to evaporate and the PU film (≈0.5 mm) to solidify (step 4). After solidification of the film, the PU was slowly peeled off of the glass substrate along with the PEDOT:OTs/PU electrodes (step 5). In parallel to the fabrication of the PEDOT:OTs/PU electrodes, the pneumatic channels and inflatable pockets were fabricated by pouring Ecoflex prepolymer into a 3D-printed mold (step 6). The same step was repeated for the planar base (no relief structures). The top layer patterned with the pneumatic elements and the planar base were then removed from their respective molds (step 7). The base layer, pneumatic top layer, and PEDOT:OTs/PU on a PU substrate were laminated by applying a thin coat of Ecoflex prepolymer between the three layers (step 8). The PEDOT:OTs/PU electrodes were addressed with copper wires and silver paste to connect to a power source.

We were not surprised to find that the mechanical response of the composite electrodes was highly dependent on the loading fraction of PU. **Figure 3**a shows representative stress–strain responses of samples containing 2.5, 5.0, and 10 wt% PU. The data were obtained by performing a horizontal pull test of the film floating on the surface of water,[32–34] and the stress was calculated using the thickness as determined by scanning electron microscopy (Figure S1, Supporting Information). As can be seen, the films with the greatest fraction of PU exhibit the greatest extensibility and lowest moduli. Films were then transferred to PDMS and subjected to uniaxial stretching while recording continuous measurements of electrical resistance (representative plots shown in Figure 3b). Notably, the films were less fragile when bonded to PDMS than they were when supported only by water as in Figure 3a (i.e., when free-standing, the films bifurcated before reaching 10% strain, whereas when bonded to PDMS, they maintained electrical continuity beyond 20%). Overall, electrical sensitivity to strain decreased as loading fraction of PU increased. In terms of baseline electrical performance, each doubling of the loading fraction of the insulating PU decreased the conductivity by more than one order of magnitude. For example, films with loading fractions of 2.5, 5.0, and 10.0 wt% PU exhibited conductivities of 27, 1.6, and 0.075 S cm^{-1} (film thicknesses were 360 nm, 415 nm, and 1.02 µm, respectively). Despite the relatively low conductivity of the blend containing 10 wt% PU, we sacrificed conductivity for mechanical softness and insensitivity of electrical resistance to strain, and thus used this blend for all subsequent experiments.

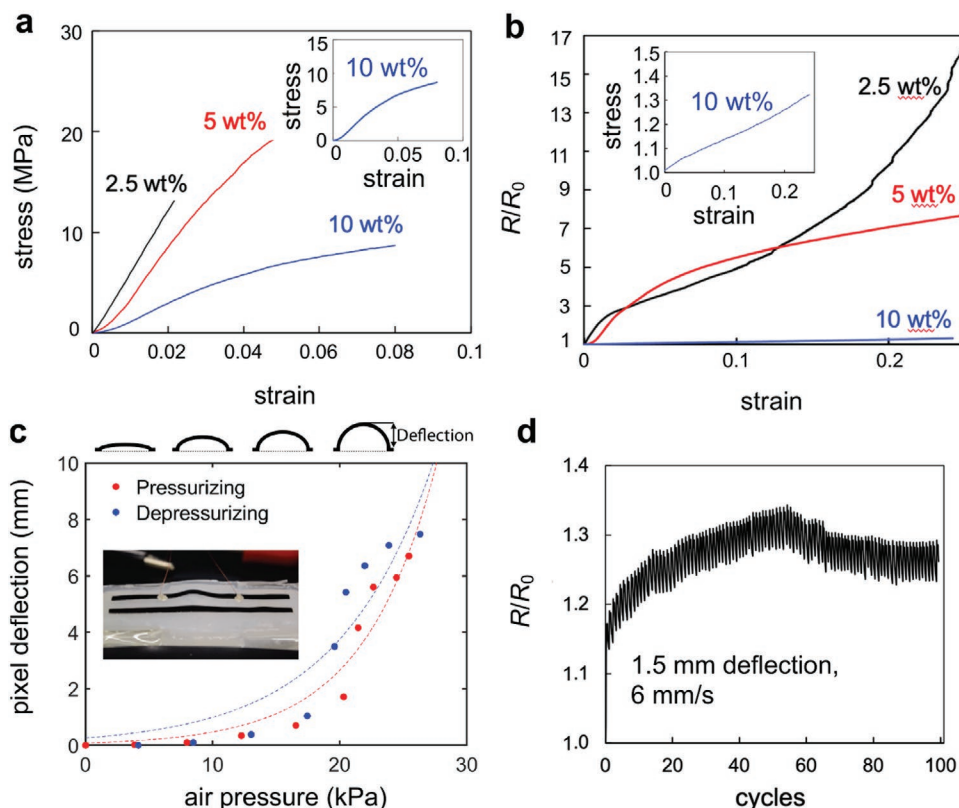We then bonded strips of the PEDOT:OTs/PU films over pneumatic pockets to mimic the geometry of the

Figure 3. Electromechanical characterization of PEDOT:OTs/PU electrodes. a) Stress–strain response of PEDOT:OTs with 2.5, 5, and 10 wt% PU. Mechanical testing of thin films was performed using the film-on-water technique.[32–34] b) Normalized resistance as a function of strain for polymer blends with different loading fractions of PU. c) Deflection as a function of air pressure corresponding to a complete pressurization cycle of one pneumatic pixel achieved by injecting and withdrawing air in increments of fixed volume. d) Normalized change in resistance of PEDOT:OTs/PU on a PU substrate during cyclic loading.

**ADVANCED
SCIENCE NEWS**

www.advancedsciencenews.com

**ADVANCED
MATERIALS
TECHNOLOGIES**

www.advmattechnol.de

electropneumotactile actuators. In order to determine the relationship between pressure and deflection, we inserted a pressure gauge in line and measured the height of an air-filled pocked upon inflation. Figure 3c shows the pixel deflection as a function of gauge pressure obtained by injecting air at fixed-volume increments. The maximum deflection rate occurred with pressures of between 20 and 23 kPa. We also observed that the height of the pixel lagged while depressurizing. This lag is visible as an offset of the blue curve from the red curve in Figure 3c. These pressures and deflections were found to be similar to those predicted by the finite element analysis. Pneumatic actuators are expected to undergo many cycles of inflation when used as a haptic device; therefore, we measured the electrical properties of the PEDOT:OTs/PU (10 wt%) overlayer under cyclic strain. Figure 3d shows the change in resistance of PEDOT:OTs/PU on a PU substrate as it was strained 1.5 mm out-of-plane at a rate of 6 mm s^{-1} for 100 cycles. These parameters were chosen to mimic the deflection and rate of inflation of a pocket during the experiments with human participants. The resistance oscillated between ≈20% and ≈35% above the initial resistance as the PEDOT:OTs/PU film was deformed out-of-plane.

To understand the baseline performance of PEDOT:OTs/PU as an electrotactile stimulator in its unstrained state, we conducted a series of human subject experiments. First, we sought to determine the minimum voltage necessary for the participants to experience stimulation (i.e., the detection threshold). The magnitude of the stimulating voltage required to induce a sensation depends largely on the impedance of the skin that varies between participants depending on skin hydration and sweat levels.[13,14] Each participant washed their hands with soap and dried their hands immediately before and after the experiment. **Figure 4**a (left) shows the experimental setup used to measure the sensitivity to electrotactile stimulation of two blindfolded participants. A function generator was used to generate an electrical signal—cathodic first, biphasic square wave with a 50% duty cycle (i.e., net-zero direct current)[13]—which was passed through a linear amplifier that multiplied the signal 20×. A ground electrode was positioned on the palm (on the muscle at the base of the thumb) of each participant. The participants made contact with a thin film of PEDOT:OTs/PU on

glass with their fingertips. Under their own control, participants increased the voltage by 2 V increments and reported when they felt a slight tingling in their fingertip. The minimum voltage required to induce a tingling sensation was reported for frequencies between 1 Hz and 1 kHz (Figure 4a, left). The voltage required for stimulation significantly decreased as the frequency increased from 1 to 100 Hz and began to level out between 100 Hz and 1 kHz. The voltage required for stimulation is initially high and then drops due to a skin capacitance effect.[20]

The manner in which electrotactile electrodes are arranged can affect the voltage required to induce stimulation as well as the resolution. There are two possible configurations of electrodes: monopolar and bipolar. A monopolar configuration has a large separation distance between the stimulating electrode and the ground electrode, while a bipolar electrode configuration places each electrode closer to one another. In our experiments, a monopolar configuration was chosen because it requires a lower voltage to induce stimulation.[13] Bipolar designs can lead to better spatial resolution but require large stimulating voltages.[35] Monopolar stimulation requires lower voltages but leads to a loss in spatial resolution. The lower voltage requirement observed in monopolar configuration manifests from electric field lines reaching deeper beneath the skin and interacting more strongly with nerves.[35]

Figure 4b shows a 2 × 2 array of PEDOT:OTs/PU electrotactile stimulators and the accuracy of five blindfolded participants when asked to identify the location of electrotactile stimulation. The same monopolar electrode configuration and frequency of electrical stimulation (100 Hz) used in Figure 4a were used in this experiment. The experiment began by calibrating the voltage supplied to each pixel. During the calibration step, subjects were asked to report the onset of electrotactile stimulation for each pixel as the experimenter steadily increased the voltage. The voltage at the onset of electrotactile stimulation was recorded for each of the four pixels. The maximum of the four voltages was used across all pixels to ensure sufficient current (≈0.4–0.5 mA) was delivered by each pixel to the fingertip. Following the calibration step, participants were asked to identify the position of electrotactile stimulation. To quantify the performance of the participants, we fit a logistic mixed effects regression model with accuracy (correct vs incorrect)
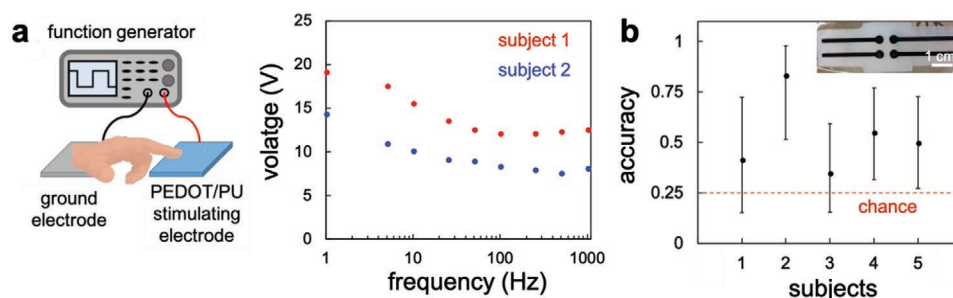

Figure 4. Calibration of the parameters used for electrotactile stimulation and psychophysical experiments. a) (left) Physical setup used to deliver controlled electrotactile stimulation to the fingertip including a function generator to deliver alternating current (charge-balanced, biphasic, square wave) between an electrode on the palm and a thin film of PEDOT:OTs/PU on a glass substrate. a) (right) Individual human subject responses to the minimum voltage required to induce a sensation at a particular frequency. b) Individual subject accuracy when discriminating between the location of one of four electrotactile pixels when energized. Error bars are 95% confidence intervals (Clopper–Pearson method for exact binomial confidence intervals).[38] The red dotted line depicts chance performance (25% accuracy). Inset: Four electrotactile pixels on an electropneumotactile device used to deliver stimulation to the fingertip of a participant.

as the dependent variable and participant as a random effect. On average, participants chose the correct location of electrical stimulation 51.7% of the time (95% confidence interval (38.7%, 64.6%)). This accuracy is significantly higher accuracy than the 25% that would be expected by chance (Wald $z = 4.32$, $p < 0.0001$). Figure 1 depicts accuracy at the participants level; note that although participants in general performed above chance, there were two subjects for which there is not statistically significant evidence of above-chance accuracy.

To assess the ability of the participants to perceive mechanical and electrical stimuli at the same time, we integrated a fluidic control board (Soft Robotics toolkit) with the function generator and linear amplifier (Figure S1, Supporting Information). The fluidic control board controlled the position and amplitude of pneumatic stimulation with a pump, four pressure sensors, and four valves. A series of mechanical relay switches controlled the position of the electrotactile stimulation. Finally, an Arduino microcontroller and custom code were used to control the location of both forms of stimulation. **Figure 5**a shows the pneumatic and electrotactile actuator positions used for human subject testing. Figure 5b shows the individual accuracy of two participants who were asked to identify the position of pneumatic stimulation between four pixels. Both participants correctly identified the position of the inflated pockets with 100% accuracy.

While participants demonstrated the ability to identify both electrical (Figure 4b) and mechanical (Figure 5b) stimuli independently, it is unclear from these results alone whether participants were able to perceive both stimuli at the same time.

Figure 5c shows the combined results of two subjects who were blindfolded and asked to determine the location (pixel #1–4) of pneumatic stimulation and whether there was electrotactile stimulation (yes/no). In the case where electrotactile stimulation was on, the location of electrotactile stimulation always coincided with the pneumatic pixel that was inflated. The results show that both participants correctly identified the combined stimuli at rates significantly higher than chance. Results of individual participants are broken down in Figure 5d,e. Figure 5f shows the number count of error types (horizontal, vertical, or both) that subjects made. A vertical error is characterized between confusing pixel #1 for #3 or pixel #2 for #4 (and vice versa), while a horizontal error was the result of subjects confusing pixel #1 for #2 or pixel #3 for #4 (and vice versa) (Figure 5a). Qualitatively, participants made errors in the vertical position (23 errors) more than in the horizontal position (14 errors). In addition, participants rarely made both errors simultaneously (four errors). This difference was statistically significant (χ^2 (2) = 13.22, $p = 0.0013$). Figure 5g depicts the residuals of the chi-squared test. Residuals larger than 2 indicate a statistically significant contribution to the overall chi-squared statistic,[36] suggesting that subjects made more vertical errors than expected, and also fewer simultaneous (horizontal and vertical) errors than would be expected if each error type were equally likely.

In this work, we introduced an electropneumotactile device that delivers multimodal haptic stimulation. Dual delivery of mechanical and electrical stimulation is achieved by combining a compliant stretchable conductor with a pneumatic actuator.
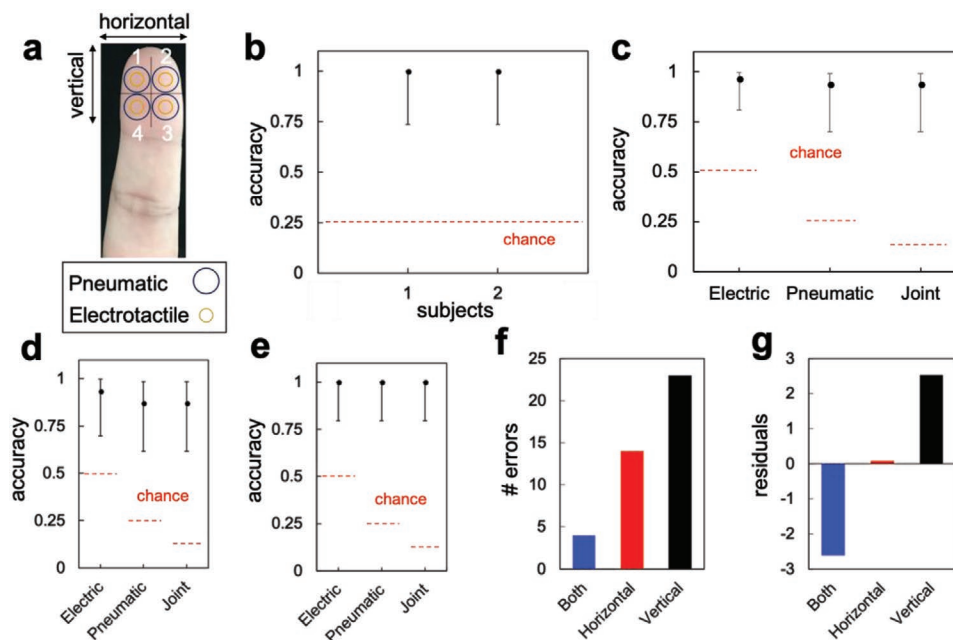

Figure 5. Psychophysical experiments using the electropneumotactile device. a) Diagram of electrotactile and pneumatic pixel locations on the fingertip. b) Individual subject accuracy when discriminating between four pneumatic pixels. Error bars are 95% confidence intervals (Clopper–Pearson method for exact binomial confidence intervals). c) Overall accuracy for human subject perception of electrotactile (electric) stimulators and pneumatic actuators, and for joint performance (correct only if subject judged both stimulation types correctly). Error bars are Wald 95% confidence intervals on fixed effects of logistic mixed effect regression model. Red line depicts chance performance. d) First subject's performance and e) second subject's performance. Error bars are 95% confidence intervals (Clopper–Pearson method for exact binomial confidence intervals). The red dotted line depicts chance performance. f) Counts of each type of error g) depiction of the residuals of the χ^2 test.

While pneumatic actuators and electrotactile electrodes are common forms of stimulation in haptic research, these two modalities have not been previously combined. We suspect this deficiency in the literature is due to the difficulty in obtaining a stretchable conductor to place on top of an inflatable actuator. The use of a highly plasticized form of the well-known conductive polymer PEDOT largely overcomes this difficulty, but at least four challenges remain. 1) In our experiments, it was difficult for participants to distinguish scenarios in which the pneumatic and electrotactile stimulation occurred at the same time but in different locations. 2) Electrotactile devices lack realism: the tingling sensation does not produce an impression in consciousness similar to the feeling of a natural material. 3) The device we describe suffers from one of the same limitations as myriad, other pneumatic tactile arrays previously described, namely selective control of inflation and deflation of each bubble. This complexity can be managed for a small array but has hindered the development denser arrays. 4) The conductive polymer is stretchable, but not especially tough; it may rub off upon repeated interrogation. However, substantial work has been done with single-[37] and multicomponent[24] PEDOT-based materials to make them significantly more mechanically resilient than the PEDOT:OTs/PU blend used here. We believe that such challenges could be addressed by further development of conductive, stretchable, and stimuli-responsive polymers.

Supporting Information

Supporting Information is available from the Wiley Online Library or from the author.

Conflict of Interest

The authors declare no conflict of interest.

[1] T. S. Hansen, K. West, O. Hassager, N. B. Larsen, *Adv. Funct. Mater.* **2007**, *17*, 3069.

[2] C. W. Carpenter, S. T. M. Tan, C. Keef, K. Skelil, M. Malinao, D. Rodriquez, M. A. Alkhadra, J. Ramírez, D. J. Lipomi, *Sens. Actuators, A* **2019**, *288*, 79.

[3] C. W. Carpenter, C. Dhong, N. B. Root, D. Rodriquez, E. E. Abdo, K. Skelil, M. A. Alkhadra, J. Ramirez, V. S. Ramachandran, D. J. Lipomi, *Mater. Horiz.* **2018**, *5*, 70.

[4] C. Dhong, L. V. Kayser, R. Arroyo, A. Shin, M. Finn, A. T. Kleinschmidt, D. J. Lipomi, *Soft Matter* **2018**, *14*, 7483.

[5] C. Dhong, R. Miller, N. B. Root, S. Gupta, L. V. Kayser, C. W. Carpenter, K. J. Loh, V. S. Ramachandran, D. J. Lipomi, *Sci. Adv.* **2019**, *5*, eaaw8845.

[6] V. Yem, H. Kajimoto, *2017 IEEE Virtual Reality*, IEEE, Piscataway, NJ **2017**, p. 99.

[7] S. Hasegawa, M. Konyo, K. Kyung, T. Nojima, H. Kajimoto, *Haptic Interaction: Science, Engineering and Design*, Springer, Singapore **2018**.

[8] S. Biswas, Y. Visell, *Adv. Mater. Technol.* **2019**, *4*, 1900042.

[9] C. W. Soule, N. Lazarus, *Smart Mater. Struct.* **2016**, *25*, 075040.

[10] Y. Qiu, Z. Lu, Q. Pei, *ACS Appl. Mater. Interfaces* **2018**, *10*, 24807.

[11] H. Kwon, S. W. Lee, S. S. Lee, *Sens. Actuators, A* **2009**, *154*, 238.

[12] N. Besse, S. Rosset, J. J. Zarate, H. Shea, *Adv. Mater. Technol.* **2017**, *10*, 1700102.

[13] D. R. Merrill, M. Bikson, J. G. R. Jefferys, *J. Neurosci. Methods* **2005**, *141*, 171.

[14] K. A. Kaczmarek, J. G. Webster, P. Bach-y-Rita, W. J. Tompkins, *IEEE Trans. Biomed. Eng.* **1991**, *38*, 1.

[15] K. A. Kaczmarek, *Sci. Iran., Trans. D* **2011**, *18*, 1476.

[16] M. Štrbac, M. Belić, M. Isaković, V. Kojić, G. Bijelić, I. Popović, M. Radotić, S. Došen, M. Marković, D. Farina, T. Keller, *J. Neural Eng.* **2016**, *13*, 046014.

[17] S. Dosen, M. Markovic, M. Strbac, M. Beli, G. Bijeli, T. Keller, D. Farina, S. Member, *IEEE Trans. Neural Syst. Rehabil. Eng.* **2017**, *25*, 183.

[18] M. Franceschi, L. Seminara, S. Dosen, M. Strbac, M. Valle, D. Farina, S. Member, *IEEE Trans. Haptics* **2017**, *10*, 162.

[19] K. A. Sluka, D. Walsh, *J. Pain* **2003**, *4*, 109.

[20] M. Ying, A. P. Bonifas, N. Lu, Y. Su, R. Li, H. Cheng, A. Ameen, Y. Huang, J. A. Rogers, *Nanotechnology* **2012**, *23*, 344004.

[21] S. Rosset, O. A. Araromi, S. Schlatter, H. R. Shea, *J. Visualized Exp.* **2016**, e53423.

[22] S. Lim, D. Son, J. Kim, Y. B. Lee, J. Song, S. Choi, D. J. Lee, J. H. Kim, M. Lee, T. Hyeon, D. Kim, *Adv. Funct. Mater.* **2015**, *25*, 375.

[23] S. E. Root, C. W. Carpenter, L. V. Kayser, D. Rodriquez, D. M. Davies, S. Wang, S. T. M. Tan, Y. S. Meng, D. J. Lipomi, *ACS Omega* **2018**, *3*, 662.

[24] L. V. Kayser, D. J. Lipomi, *Adv. Mater.* **2019**, *31*, 1806133.

[25] J. Y. Oh, S. Kim, S. Baik, U. Jeong, *Adv. Mater.* **2016**, *28*, 4455.

[26] L. V. Kayser, M. D. Russell, D. Rodriquez, S. N. Abuhamdieh, C. Dhong, S. Khan, A. N. Stein, J. Ram, D. J. Lipomi, *Chem. Mater.* **2018**, *30*, 4459.

[27] D. Khodagholy, T. Doublet, M. Gurfinkel, P. Quilichini, E. Ismailova, P. Leleux, T. Herve, S. Sanaur, C. Bernard, G. G. Malliaras, *Adv. Mater.* **2011**, *23*, H268.

ADVANCED
SCIENCE NEWS

www.advancedsciencenews.com

ADVANCED
MATERIALS
TECHNOLOGIES

www.advmattechnol.de

[28] M. Sessolo, D. Khodagholy, J. Rivnay, F. Maddalena, M. Gleyzes, E. Steidl, B. Buisson, G. G. Malliaras, *Adv. Mater.* **2013**, *25*, 2135.

[29] D. Khodagholy, J. N. Gelinas, Z. Zhao, M. Yeh, M. Long, J. D. Greenlee, W. Doyle, O. Devinsky, G. Buzsáki, *Sci. Adv.* **2016**, *2*, e1601027.

[30] M. Ganji, E. Kaestner, J. Hermiz, N. Rogers, A. Tanaka, D. Cleary, S. H. Lee, J. Snider, M. Halgren, G. R. Cosgrove, B. S. Carter, D. Barba, I. Uguz, G. G. Malliaras, S. S. Cash, V. Gilja, E. Halgren, S. A. Dayeh, *Adv. Funct. Mater.* **2018**, *12*, 1700232.

[31] X. Crispin, F. L. E. Jakobsson, A. Crispin, P. C. M. Grim, P. Andersson, A. Volodin, C. van Haesendonck, M. Van der Auweraer, W. R. Salaneck, M. Berggren, *Chem. Mater.* **2006**, *18*, 4354.

[32] J. Kim, A. Nizami, Y. Hwangbo, B. Jang, H. Lee, C. Woo, S. Hyun, T. Kim, *Nat. Commun.* **2013**, *4*, 2520.

[33] D. Rodriquez, J. Kim, S. E. Root, Z. Fei, P. Bou, M. Heeney, T. Kim, D. J. Lipomi, *ACS Appl. Mater. Interfaces* **2017**, *9*, 8855.

[34] M. A. Alkhadra, S. E. Root, K. M. Hilby, D. Rodriquez, F. Sugiyama, D. J. Lipomi, *Chem. Mater.* **2017**, *29*, 10139.

[35] P. Comte, *Appl. Neurophysiol.* **1982**, *45*, 156.

[36] P. L. MacDonald, R. C. Gardner, *Educ. Psychol. Meas.* **2000**, *60*, 735.

[37] L. V. Kayser, M. D. Russell, D. Rodriquez, S. N. Abuhamdieh, C. Dhong, S. Khan, A. N. Stein, J. Ramírez, D. J. Lipomi, *Chem. Mater.* **2018**, *30*, 4459.

[38] C. J. Clopper, E. S. Pearson, *Biometrika* **1934**, *26*, 404.